Magnetoplasmon polaritons and resonant optical transmission of a finite random-thickness superlattice in a magnetic field

1995 J. Phys.: Condens. Matter 7 3431

(http://iopscience.iop.org/0953-8984/7/18/007)

J. Phys.: Condens. Matter 7 (1995) 3431–3444. Printed in the UK

Magnetoplasmon polaritons and resonant optical transmission of a finite random-thickness superlattice in a magnetic field

Shi-Jie Xiong and Rong-Bo Ou-Yang

Department of Physics and Solid Microstructure Laboratory, Nanjing University, Nanjing 210008, People's Republic of China

Received 29 December 1994, in final form 2 March 1995

Abstract. We investigate the magnetoplasmon polariton modes and the propagation of electromagnetic waves in a random-thickness superlattice in a magnetic field. The layer thicknesses are distributed in accordance with a special probability function. The magnetic field is parallel to the interfaces, and the propagation of the waves is perpendicular to the field. By use of the transfer-matrix method we show that there exists a resonant optical transmission for waves with particular frequencies. We calculate the dispersion relation of the bulk modes, the resonant frequencies and the transmission coefficients. The transmission coefficients at the resonant frequencies are sensitive to variations in the magnetic field. Possible applications of such a structure in new devices are discussed.

1. Introduction

Recently, the spectra of electrons and the optical properties of superlattices with randomly distributed layer thicknesses have been studied both theoretically and experimentally [1–4]. Because the optical and transport properties of a superlattice depend on its tailored structure, i.e. on the compositions and the layer thicknesses, the artificially designed randomness in thicknesses provides new possibilities of applications in optical and electronic devices. As the random thicknesses violate Bloch symmetry in the growth direction, the fundamental miniband structure of a random superlattice is much more complicated than a periodic superlattice. This may lead to some unusual optical properties, for example optical absorption and luminescence. On the other hand, if the interfaces are smooth enough that the wave vector parallel to the laminations, $k_{\parallel}$, is preservative, the propagation along the growth direction of an elementary excitation with a given $k_{\parallel}$ can be viewed as the corresponding motion in a one-dimensional (1D) disordered system. In accordance with scaling theory [5], most of the states of the excitation in such a 1D system are localized, owing to the randomness. For several types of random 1D structures, however, it has been proved that there still exist completely unscattered states [6]. This feature can cause unusual resonant tunneling of electrons [7] or resonant transmission of acoustic waves in such random superlattices.

Collective plasmon polaritons in superlattices with regular layer thicknesses have been investigated extensively [8–13]. It is interesting to investigate the relationship between the behaviour of the excitations and the structure of the superlattices. Camley and Mills have demonstrated that in a semi-infinite superlattice the existence of a surface-plasmon mode depends on the ratio of the layer thicknesses [14]. Johnson and co-workers have found that surface-plasmon modes in a finite superlattice can be localized to the top and

0953-8984/95/183431+14$19.50

bottom surfaces by slightly changing the dielectric constant of the gaps in the structure [15]. From a calculated example presented by Johnson and Camley, the dispersion relation of plasmons in a finite superlattice (ten layers) seems to be not particularly sensitive to the fluctuation of thickness of a single layer [16]. We have calculated the properties of plasmon polaritons in a finite n–i–p–i superlattice with layer thicknesses randomly distributed in accordance with uniform probabilities and found that, in varying the degree of randomness, the frequencies of bulk modes only shift slightly, which is consistent with the result of [16], but the transmission coefficients are remarkably changed [17].

Similar to the propagation of electrons and phonons, in special random superlattices there also exists resonant transmission for electromagnetic (EM) waves at distinctive frequencies. In this paper we introduce particular probabilities for the distribution of random layer thicknesses of a superlattice consisting of alternate deposition of conductive and insulating layers and determine the resonant frequencies at which the EM waves are completely unscattered by the randomness. We subject finite samples of such a structure to an external magnetic field parallel to the laminations, and suppose that the incident plane of the waves is perpendicular to the field. In varying the degree of randomness, the strength of the field, and the total number of layers, we calculate the dispersion relations of the magnetoplasmon polariton modes and the transmission coefficients of the EM waves. In the calculations we assume that the thicknesses are all large enough that every film can be characterized by a macroscopic dielectric function. The discontinuities at the interfaces are treated by the transfer-matrix method. We show that in a finite sample the variations of the degree of randomness and the magnetic field cause only a slight shift of the frequencies of the bulk modes, but large changes in the transmission characteristics. In particular, the resonant peaks are rapidly sharpened as the degree of randomness increases, and their frequencies are shifted when the magnetic field is changed. We also show that the transmission coefficient at a resonant frequency is rapidly damped if the magnetic field is slightly increased. All these characteristics provide the possibility of developing new electro-optical devices.

The paper is organized as follows. In section 2 we describe the structure of the random superlattices investigated in this paper and the formalism of the transfer-matrix method. In section 3 we calculate the dispersion relations of the magnetoplasmon polaritons and the resonant frequencies for the propagation of the EM waves. In section 4 we present the results of the calculated transmission coefficients as a function of frequency and magnetic field for finite samples with different total numbers of layers. Finally, we summarize the results in section 5.

2. Model and transfer-matrix formalism

We consider a superlattice consisting of alternating layers of materials, which we label A and B. A is assumed to be an insulator, and B is assumed to be a material containing charge carriers. The total number of layers is finite. The random layered structure investigated in this paper can be viewed as that constructed by randomly inserting a number of identical units, each of which is an alternating array of m layers of material A with thickness L_a and m layers of material B with thickness L_b, into a uniform slab of material A, with all of the interfaces parallel to the surfaces of the slab (see figure 1). We can use the following array of layers to describe the whole system:

$$A_1B_1A_2B_2\cdots A_iB_i\cdots A_NB_NA_{N+1} \tag{1}$$

where A_i ($i = 1, 2, \ldots, N, N+1$) represent layers of species A with partially random thicknesses l_{ai}, and B_i ($i = 1, 2, \ldots, N$) represent layers of species B with a regular thickness L_b. The thicknesses l_{ai} satisfy the following probability distribution:

$$p(l_{ai}) = (1 - \delta_{i,nm+1})\delta(l_{ai} - L_a) + \frac{\delta_{i,nm+1}\theta(l_{ai} - d_1)\theta(d_2 - l_{ai})}{d_2 - d_1} \tag{2}$$

where $\delta(x)$ is the usual δ function, and

$$\delta_{i,nm+1} = \begin{cases} 0 & i \neq nm+1 \\ 1 & i = nm+1 \end{cases} \qquad \theta(x) = \begin{cases} 0 & x < 0 \\ 1 & x \geqslant 0 \end{cases}$$

with $n = 0, 1, 2, \ldots, M$ and $N = Mm$.

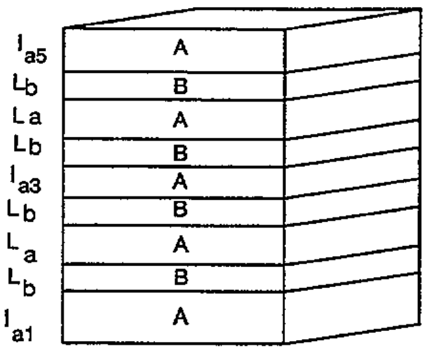

Figure 1. Structure of a superlattice with partially random layer thicknesses of species A and regular layer thicknesses of species B; $m = 2$ and $l_{a1}, l_{a3}, l_{a5} \ldots$ are randomly distributed.

Such a structure is similar to the random multibarrier superlattice considered in [7], but now the 'barrier' is a conductive layer and the 'well' is an insulating layer. One 'multibarrier' consists of m conductive layers separated by the insulating layers, and there are M 'multibarriers' in the whole system. We let the left surface of the superlattice lie in the x–z plane. A static magnetic field is applied along the z axis. In this paper we restrict ourselves to the magnetoplasmon polariton modes propagating in the x–y plane.

We start with the general wave equation for the electric field ($\boldsymbol{E}$) in terms of the macroscopic dielectric tensor $\hat{\epsilon}$:

$$\nabla \times (\nabla \times \boldsymbol{E} - q_0^2\, \hat{\epsilon} \boldsymbol{E}) = 0 \tag{3}$$

where $q_0 = \omega/c$, ω is the frequency of the wave and c is the velocity of light. Within an insulating layer, $\hat{\epsilon}$ reduces to a scalar:

$$\hat{\epsilon} = \epsilon_a \hat{1} \tag{4}$$

where $\hat{1}$ is a unit tensor. In a conductive film, we have the following expression for $\hat{\epsilon}$:

$$\hat{\epsilon} = \begin{pmatrix} \epsilon_1 & -i\epsilon_2 & 0 \\ i\epsilon_2 & \epsilon_1 & 0 \\ 0 & 0 & \epsilon_3 \end{pmatrix} \tag{5}$$

where

$$\epsilon_1 = \epsilon_b \left(1 + \frac{\omega_p^2(\omega + i/\gamma)}{\omega[\omega_c^2 - (\omega + i/\gamma)^2]} \right) \tag{6}$$

$$\epsilon_2 = \epsilon_b \frac{\omega_c \omega_p^2}{\omega[\omega_c^2 - (\omega + i/\gamma)^2]} \tag{7}$$

$$\epsilon_3 = \epsilon_b \left(1 - \frac{\omega_p^2}{\omega(\omega + i\gamma)} \right). \tag{8}$$

Here ϵ_b is the background dielectric constant, ω_p is the plasma frequency, γ is the relaxation time of carriers, and ω_c is the cyclotron frequency eB/m^*c, with B and m^* being the magnetic field strength and the effective mass of the charge carriers, respectively. For most conductors the damping rate of the carriers $(1/\gamma)$ is much smaller than the frequency of visible light. So we can assume $1/\gamma$ to be zero if we are mainly interested in light with a frequency higher than $1/\gamma$. As the waves are propagating within the x–y plane, by assuming plane-wave solutions of $\boldsymbol{E}$ we obtain the wave equation appropriate to material A:

$$\begin{pmatrix} q_0^2\epsilon_a - k_{ya}^2 & k_x k_{ya} & 0 \\ k_x k_{ya} & q_0^2\epsilon_a - k_x^2 & 0 \\ 0 & 0 & q_0^2\epsilon_a - k_x^2 - k_{ya}^2 \end{pmatrix} \boldsymbol{E} = 0 \tag{9}$$

and the equation for material B:

$$\begin{pmatrix} q_0^2\epsilon_1 - k_{yb}^2 & k_x k_{yb} + i q_0^2 \epsilon_2 & 0 \\ k_x k_{yb} - i q_0^2\epsilon_2 & q_0^2\epsilon_1 - k_x^2 & 0 \\ 0 & 0 & q_0^2\epsilon_3 - k_x^2 - k_{yb}^2 \end{pmatrix} \boldsymbol{E} = 0 \tag{10}$$

where k_x is the x component of the wave vector, and k_{ya} and k_{yb} are its y components in materials A and B, respectively. Note that ω and k_x are preserved across the interfaces. The relationships among ω, k_y and k_x are determined by setting the determinants of the coefficient matrices in (9) and (10) to be zero, and the results are

$$k_{ya}^2 = \epsilon_a q_0^2 - k_x^2 \tag{11}$$

and

$$k_{yb}^2 = \begin{cases} k_{y1}^2 \equiv \epsilon_3 q_0^2 - k_x^2 & z \text{ component of } \boldsymbol{E} \text{ (s polarization)} \\ k_{y2}^2 \equiv (\epsilon_1^2 - \epsilon_2^2) q_0^2/\epsilon_1 - k_x^2 & x,\ y \text{ components of } \boldsymbol{E} \text{ (p polarization).} \end{cases} \tag{12}$$

The x and y components of $\boldsymbol{E}$ are related by

$$E_y = -\frac{k_x}{k_{ya}} E_x \quad \text{for material A} \tag{13}$$

$$E_y = \frac{k_{y2}^2 - q_0^2\epsilon_1}{i q_0^2 \epsilon_2 + k_x k_{y2}} E_x \quad \text{for material B.} \tag{14}$$

The general form of the wave solutions in the ith layer of materials A and B can be expressed in terms of a superposition of waves with k_y and $-k_y$:

$$E_x(x, y) = \{A_{i1}^{(x)} \exp[ik_{ya}(y - y_{ia})] + A_{i2}^{(x)} \exp[-ik_{ya}(y - y_{ia})]\} \exp(ik_x x) \tag{15}$$

$$E_z(x, y) = \{A_{i1}^{(z)} \exp[ik_{ya}(y - y_{ia})] + A_{i2}^{(z)} \exp[-ik_{ya}(y - y_{ia})]\} \exp(ik_x x) \tag{16}$$

for the ith layer of species A, and

$$E_x(x, y) = \{B_{i1}^{(x)} \exp[ik_{y2}(y - y_{ib})] + B_{i2}^{(x)} \exp[-ik_{y2}(y - y_{ib})]\} \exp(ik_x x) \tag{17}$$

$$E_z(x, y) = \{B_{i1}^{(z)} \exp[ik_{y1}(y - y_{ib})] + B_{i2}^{(z)} \exp[-ik_{y1}(y - y_{ib})]\} \exp(ik_x x) \tag{18}$$

for the ith layer of species B. Here y_{ia} (or y_{ib}) is the coordinate of the interface between layer A_i (or B_i) and its preceding layer in (1). The standard EM boundary conditions at the interfaces between A and B layers are the continuity of the tangential electric- and magnetic-field components: E_x, E_z, B_x and B_z. We suppose that in the materials A and B the susceptibility μ is unity, so the magnetic field $\boldsymbol{B}$ can be written in terms of $\boldsymbol{E}$ via Faraday's law: $\nabla \times \boldsymbol{E} = iq_0\mathbf{B}$. For the present geometry, E_x and E_y are decoupled from E_z, so one has two independent boundary conditions for E_x or E_z at an interface. We express them in a 2×2 matrix form:

$$\mathbf{P}\mathbf{R}_{ia} \begin{pmatrix} A_{i1}^{(\nu)} \\ A_{i2}^{(\nu)} \end{pmatrix} = \mathbf{Q}^{(\nu)} \begin{pmatrix} B_{i1}^{(\nu)} \\ B_{i2}^{(\nu)} \end{pmatrix} \quad \text{at interface } y_{ib} \tag{19}$$

$$\mathbf{Q}^{(\nu)}\mathbf{R}_{b}^{(\nu)} \begin{pmatrix} B_{i-1,1}^{(\nu)} \\ B_{i-1,2}^{(\nu)} \end{pmatrix} = \mathbf{P} \begin{pmatrix} A_{i1}^{(\nu)} \\ A_{i2}^{(\nu)} \end{pmatrix} \quad \text{at interface } y_{ia} \tag{20}$$

where $\nu = x, z$, and the 2×2 matrices are defined by

$$\mathbf{P} = \begin{pmatrix} 1 & 1 \\ -i\epsilon_a/k_{ya} & i\epsilon_a/k_{ya} \end{pmatrix} \tag{21}$$

$$\mathbf{Q}^{(z)} = \begin{pmatrix} 1 & 1 \\ -i\epsilon_3/k_{y1} & i\epsilon_3/k_{y1} \end{pmatrix} \tag{22}$$

$$\mathbf{Q}^{(x)} = \begin{pmatrix} 1 & 1 \\ (-\epsilon_1 k_x - i\epsilon_2 k_{y2})/(q_0^2\epsilon_2 - ik_x k_{y2}) & (i\epsilon_2/k_{y2} - \epsilon_1 k_x)/(q_0^2\epsilon_2 + ik_x k_{y2}) \end{pmatrix} \tag{23}$$

$$\mathbf{R}_{ia} = \mathbf{R}_0 \equiv \begin{pmatrix} \exp(ik_{ya}L_a) & 0 \\ 0 & \exp(-ik_{ya}L_a) \end{pmatrix} \tag{24}$$

for $i \neq nm + 1$, $(n = 0, 1, 2, \ldots, M)$

$$\mathbf{R}_{ia} = \mathbf{R}_0\mathbf{R}_n \qquad \mathbf{R}_n = \begin{pmatrix} \exp[ik_{ya}(l_{ai} - L_a)] & 0 \\ 0 & \exp[-ik_{ya}(l_{ai} - L_a)] \end{pmatrix} \tag{25}$$

for $i = nm + 1$, and

$$\mathbf{R}_b^{(\nu)} = \begin{pmatrix} \exp(ik_{y\mu}L_b) & 0 \\ 0 & \exp(-ik_{y\mu}L_b) \end{pmatrix} \qquad \begin{cases} \mu = 1 & \nu = z \\ \mu = 2 & \nu = x. \end{cases} \tag{26}$$

In these expressions we have used the fact that the thicknesses of layers of species A are partially random, and the thicknesses of all layers of species B are regular. The amplitudes in layers A_i and A_{i+1} are related by

$$\begin{pmatrix} A^{(\nu)}_{i+1,1} \\ A^{(\nu)}_{i+1,2} \end{pmatrix} = \mathbf{T}^{(\nu)}_i \begin{pmatrix} A^{(\nu)}_{i1} \\ A^{(\nu)}_{i2} \end{pmatrix} \tag{27}$$

with

$$\mathbf{T}^{(\nu)}_i = \mathbf{T}^{(\nu)}_0 \equiv [\mathbf{P}]^{-1}\mathbf{Q}^{(\nu)}\mathbf{R}^{(\nu)}_b[\mathbf{Q}^{(\nu)}]^{-1}\mathbf{P}\mathbf{R}_0 \tag{28}$$

for $i \neq nm + 1$, and

$$\mathbf{T}^{(\nu)}_i = \mathbf{T}^{(\nu)}_0 \mathbf{R}_n \tag{29}$$

for $i = nm + 1$. Thus the relationship between the fields at the two ends of the whole system can be written as

$$\begin{pmatrix} A^{(\nu)}_{N+1,1} \\ A^{(\nu)}_{N+1,2} \end{pmatrix} = \mathbf{T}^{(\nu)} \begin{pmatrix} A^{(\nu)}_{1,1} \\ A^{(\nu)}_{1,2} \end{pmatrix} \tag{30}$$

where

$$\mathbf{T}^{(\nu)} = \prod_{n=1}^{M} [\mathbf{T}^{(\nu)}_0]^m \mathbf{R}_{M-n}. \tag{31}$$

From the definition, we can see that $\mathbf{T}^{(\nu)}_0$, $\mathbf{T}^{(\nu)}_i$, $(i = 1, 2, \ldots, N)$, and $\mathbf{T}^{(\nu)}$ are all unimodular 2×2 matrices. By using a theorem from matrix theory described in [18], one has

$$[\mathbf{T}^{(\nu)}_0]^m = u_{m-1}(\tau)\mathbf{T}^{(\nu)}_0 - u_{m-2}(\tau)\mathbf{I} \tag{32}$$

where $\tau = \frac{1}{2}\mathrm{Tr}(\mathbf{T}^{(\nu)}_0)$, $\mathbf{I}$ is a unit matrix, and $u_m(\tau)$ is the mth Chebyshev polynomial of the second kind, which obeys the recurrence relation

$$u_{m+1}(\tau) = 2\tau u_m(\tau) - u_{m-1}(\tau) \qquad m \geqslant 0 \tag{33}$$

with $u_{-1} = 0$ and $u_0 = 1$. If $|\tau| \leqslant 1$, $u_m(\tau)$ has the form

$$u_{m-1}(\tau) = \frac{\sin(m\varphi)}{\sin(\varphi)} \tag{34}$$

with $\varphi = \cos^{-1}(\tau)$.

We note that, for our geometry, the magnetic field only influences the modes of p-polarized EM waves.

3. Dispersion relation of the bulk modes and the unscattered modes

From the equations derived in the last section we can calculate the dispersion relations for the modes of magnetoplasmon polaritons with different degrees of randomness and in different magnetic fields. The randomness in layer thicknesses breaks the periodicity in the growth direction; we have to restrict ourselves to a system containing only a finite number of layers. In this paper we are only interested in the bulk modes, i.e. we look for frequencies at which the solutions of the field do not grow exponentially. In a more restricted version, similar to the standard procedure employed in investigations of quasiperiodic systems [19], we impose a Bloch ansatz on the amplitudes at the two ends of the finite system described by (1):

$$\begin{pmatrix} A^{(\nu)}_{N+1,1} \\ A^{(\nu)}_{N+1,2} \end{pmatrix} = \exp(\mathrm{i}qL) \begin{pmatrix} A^{(\nu)}_{1,1} \\ A^{(\nu)}_{1,2} \end{pmatrix} \tag{35}$$

where q is the Bloch index reflecting this periodic boundary condition, and

$$L = \sum_{n=0}^{M-1} l_{a,nm+1} + (m-1)ML_{\mathrm{a}} + mML_{\mathrm{b}}$$

is the distance between the first layer and the $(2N+1)$th layer. From (30) we have

$$\mathbf{T}^{(\nu)} \begin{pmatrix} A^{(\nu)}_{1,1} \\ A^{(\nu)}_{1,2} \end{pmatrix} = \exp(\mathrm{i}qL) \begin{pmatrix} A^{(\nu)}_{1,1} \\ A^{(\nu)}_{1,2} \end{pmatrix}. \tag{36}$$

The existence of non-trivial solutions for $A^{(\nu)}_{1,1}$ and $A^{(\nu)}_{1,2}$, together with the fact that $\mathbf{T}^{(\nu)}$ is a unimodular 2×2 matrix, leads to

$$\chi = \tfrac{1}{2}\mathrm{Tr}(\mathbf{T}^{(\nu)}) = \cos(qL) \qquad \text{or } |\chi| \leqslant 1. \tag{37}$$

The dispersion relations for s and p polarizations are calculated from this equation with $\nu = z$ and $\nu = x$, respectively. The result is a set of minibands of frequencies which meet the condition in (37). Such a miniband structure comes from the imposed Bloch ansatz, and their widths are reduced to zero in the limit $N \to \infty$. In the calculation of the dispersion relations, we employ a finite sample with N large enough that the widths of the minibands are of the same order as the frequency resolution in the figures. In the absence of a magnetic field, these two modes are degenerate. By applying the magnetic field, the s-polarized modes are unchanged, while the frequencies of the p-polarized modes are altered. In figures 2 and 3 we plot the dispersion relations for the s- and p-polarized modes in the absence of a magnetic field (also for the s-polarized modes in the presence of magnetic field) in two finite samples with $m = 2$ and $m = 3$, respectively. The results are presented here in terms of the reduced frequencies, $\omega/\omega_{\mathrm{p}}$, the reduced wave vector, ck_x/ω_{p}, and the reduced layer thickness $\omega_{\mathrm{p}}l/c$. The minibands are illustrated by the dots at several values of wave vector. It can be seen that the dots are gathered together to form several separated groups. As the sample with larger m has more regular layers, and so less randomness, in a comparison of figures 2 and 3 we can see that the change of the degree of randomness only slightly shifts the frequencies of the modes, which is consistent with the results of [16], but the sample with more randomness exhibits more structure of the miniband groups. In figures 4 and 5 we plot the dispersion relations of the p-polarized modes in the presence of

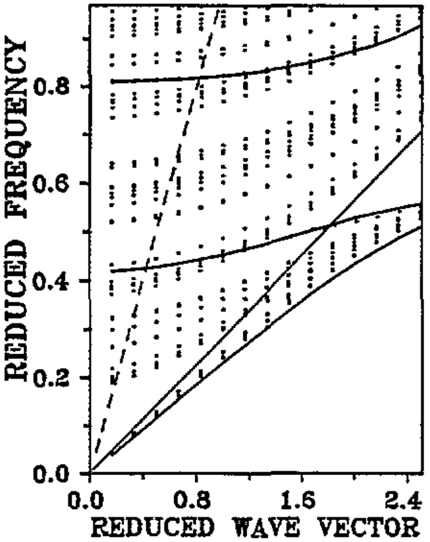

Figure 2. The dispersion relation of bulk plasmon polariton modes (represented by the dots) and the unscattered modes (represented by the full curves) of a random superlattice in the absence of a magnetic field. The parameters of the sample are: $\epsilon_a = \epsilon_b = 13.13$, $\omega_p L_a/c = 1.5$, $\omega_p L_b/c = 1.3$, $N = 20$, $m = 2$, $\omega_p d_1/c = 1.6$, $\omega_p d_2/c = 4.6$. The broken line is for $\omega = ck_x$, and the full straight line is for $\omega = ck_x\epsilon^{-1/2}$.

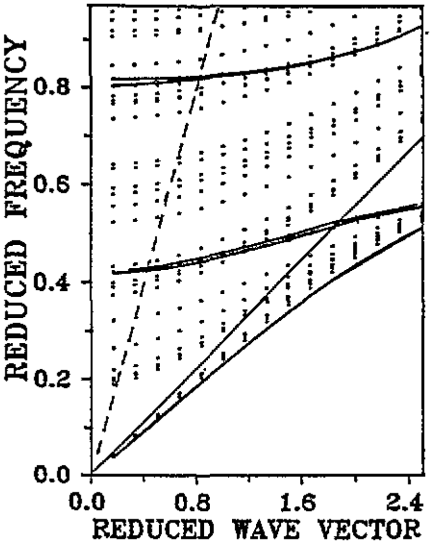

Figure 3. The dispersion relation of bulk plasmon polariton modes and the unscattered modes of a random superlattice in the absence of a magnetic field. The notations and the parameters are the same as those in figure 1, except that $m = 3$.

a magnetic field for the same samples as those in figures 2 and 3. The magnetic field is also expressed in reduced units of ω_c/ω_p. It can be seen that by applying the magnetic field the miniband-group structure of the p-polarized modes becomes more complicated, particularly near the cyclotron frequency, owing to the resonant response of the cyclotrons.

Although the bulk modes do not grow or get damped exponentially from the surfaces, most of the modes are scattered by the randomness and may be localized at some layers within the system. This is just the situation predicted by the scaling theory of a one-dimensional disordered system. In the present structure defined by (1) and (2), however, there exist some modes that are completely unscattered by the randomness. In fact, from (32) and (34) we can see that if $m \geqslant 2$ and the frequency of a mode satisfies

$$\tau = \cos(j\pi/m) \qquad j = 1, 2, \ldots, m-1 \tag{38}$$

then

$$[\mathbf{T}_0^{(\nu)}]^m = (-1)^j \mathbf{I} \tag{39}$$

and

$$\mathbf{T}^{(\nu)} = (-1)^{jM} \prod_{n=1}^{M} \mathbf{R}_{M-n}. \tag{40}$$

Since the product on the right-hand side of this equation is just the transfer matrix of a uniform slab of material A with thickness $\sum_{n=0}^{M-1} l_{a,nm+1}$, the propagation of this mode in the

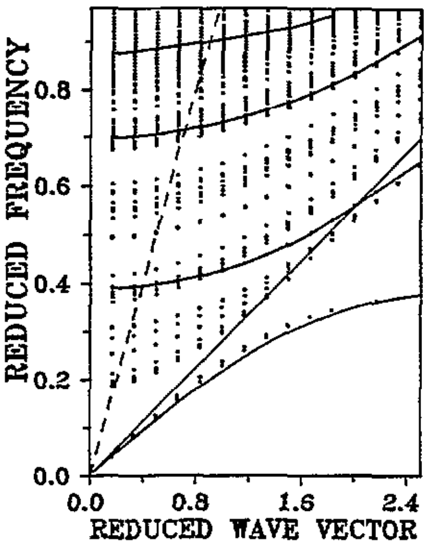

Figure 4. The dispersion relation of bulk magnetoplasmon polariton modes and the unscattered modes of a random superlattice in the presence of a magnetic field. The notations and the parameters are the same as those in figure 1 and the magnetic field is $\omega_c/\omega_p = 0.7$.

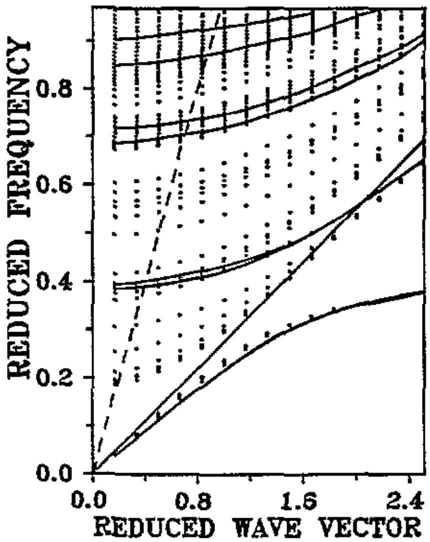

Figure 5. The dispersion relation of bulk magnetoplasmon polariton modes and the unscattered modes of a random superlattice in the presence of a magnetic field. The notations and the parameters are the same as those in figure 2 and the magnetic field is $\omega_c/\omega_p = 0.7$.

sample is similar to its propagation in a uniform medium of A, and is completely unscattered by the randomness. The dispersion relations of these unscattered modes are determined by (38) and are represented by the full curves in figures 2–5 for the corresponding samples. We can see that in the frequency region of $\omega \geqslant \epsilon_a^{1/2} k_x$ (above the straight line $k_{ya} = 0$ in the figures), these modes are within the minibands of the bulk modes. Outside this region (beneath the straight line $k_{ya} = 0$), these modes are not located within the bulk minibands. This is because the propagation of the waves in this frequency region in a uniform medium of material A is exponentially damping, so they belong to the surface modes, although they are not scattered by the randomness. By comparing these figures, one can see that when m is changed from two to three, the curves for the unscattered modes are split into double curves, as can be expected from (38). The examples of the frequencies of the unscattered p-polarized modes as a function of magnetic field and layer thickness L_a are presented in figures 6 and 7, respectively. The dividing line for the bulk modes and the surface modes is shown by a chain curve. The frequencies of the unscattered bulk modes and surface mode both decrease as the magnetic field increases, because the cyclotrons reduce the dielectric functions ϵ_1 and ϵ_2 of the conduction layers, so a compensating decrease of the unscattered frequency is required for meeting condition (38). By increasing the thickness of the insulating layers L_a, the frequencies of unscattered bulk modes are reduced but that of the surface mode is slightly increased. This is because the frequency dependences of the wavelength of a bulk mode and the damping length of a surface mode are opposite, so the compensating tendencies of their frequencies for meeting condition (38) in varying the layer thickness are also opposite.

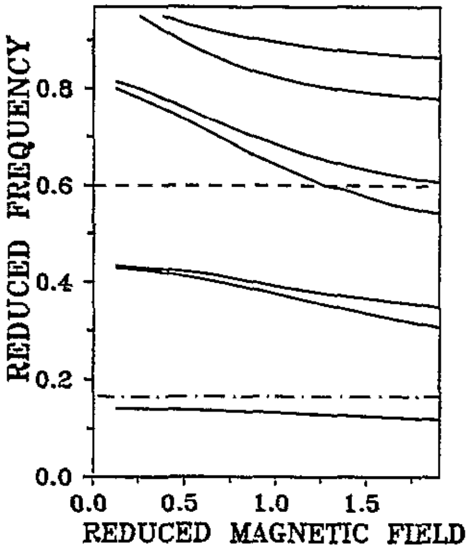

Figure 6. The frequencies of the unscattered modes as a function of the magnetic field. The parameters of the sample are the same as those of figure 2 and $k_x c/\omega_p = 0.6$. The broken line is for $\omega = ck_x$ and the chain line is for $\omega = ck_x\epsilon^{-1/2}$.

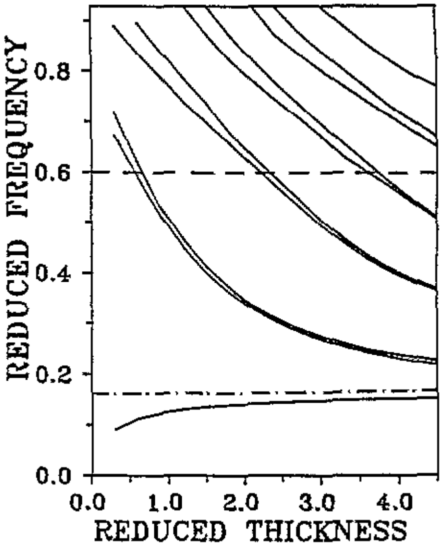

Figure 7. The frequencies of the unscattered modes as a function of the layer thickness L_a. The parameters of the sample and the wave vector are the same as those of figure 5, except L_a. The magnetic field is $\omega_c/\omega_p = 0.7$. The broken line is for $\omega = ck_x$ and the chain line is for $\omega = ck_x\epsilon^{-1/2}$.

4. High-quality resonant transmission

Since the randomness reflects most of the bulk modes except the unscattered modes mentioned above, one may expect a high-quality resonant transmission of EM waves through such a structure. We consider a finite superlattice consisting of the first N layers of species A and N layers of species B and without the $(N+1)$th layer in the series given by (1), and insert it into an infinite uniform medium of insulator C with dielectric constant ϵ_c. We assume that the incident EM wave of s- or p-polarization propagates from the left part of medium C towards the superlattice, with its wave vector in the x–y plane and an amplitude of unity. Part of the wave is reflected by the random superlattice. We denote the amplitudes of the reflected and transmitted wave by $r^{(\nu)}$ and $t^{(\nu)}$, respectively. Here $\nu = x, z$ specifies the polarization of the wave. The field components in the two parts of medium C are related to those in the superlattice by the boundary conditions at the two interfaces:

$$\begin{pmatrix} A_{1,1}^{(\nu)} \\ A_{1,2}^{(\nu)} \end{pmatrix} = \mathsf{F}_1 \begin{pmatrix} 1 \\ r^{(\nu)} \end{pmatrix} \tag{41}$$

and

$$\begin{pmatrix} t^{(\nu)} \\ 0 \end{pmatrix} = \mathsf{F}_2^{(\nu)} \begin{pmatrix} B_{N,1}^{(\nu)} \\ B_{N,2}^{(\nu)} \end{pmatrix} \tag{42}$$

where

$$\mathsf{F}_1 = \begin{pmatrix} (1+s)/2 & (1-s)/2 \\ (1-s)/2 & (1+s)/2 \end{pmatrix} \tag{43}$$

with

$$s = \left(\frac{\epsilon_c}{\epsilon_a}\right)^{1/2} \qquad \mathbf{F}_2^{(\nu)} = [\mathbf{F}_1]^{-1}[\mathbf{P}]^{-1}\mathbf{Q}^{(\nu)}\mathbf{R}_b^{(\nu)}. \tag{44}$$

By using (28), (30) and (31) we have

$$\begin{pmatrix} t^{(\nu)} \\ 0 \end{pmatrix} = \mathbf{Y}^{(\nu)} \begin{pmatrix} 1 \\ r^{(\nu)} \end{pmatrix} \tag{45}$$

where

$$\mathbf{Y}^{(\nu)} = [\mathbf{F}_1]^{-1}\mathbf{T}^{(\nu)}\mathbf{F}_1.$$

By solving this equation for $t^{(\nu)}$, one obtains the transmission coefficient

$$|t^{(\nu)}|^2 = 1/|[\mathbf{Y}^{(\nu)}]_{22}|^2. \tag{46}$$

If the frequency of a mode meets the condition (38) and is higher than $c\epsilon_a^{1/2}k_x$ and $c\epsilon_c^{1/2}k_x$, it can transmit through the whole system, just like its transmission through a slab of species A embedded in a uniform medium C. If A and C are of the same material, the transmission coefficient for this mode is unity. When A and C are different, the transmission is determined by the phase coherence between the transmitted and reflected wave at the two ends of the superlattice, depending on the sum $\sum_{n=0}^{M-1} l_{a,nm+1}$.

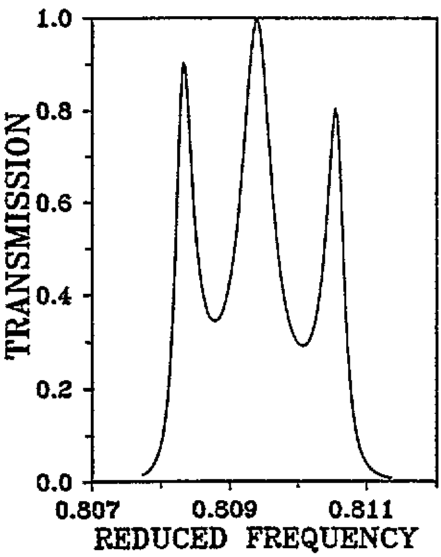

Figure 8. The transmission coefficient as a function of frequency in the absence of a magnetic field for the sample of parameters described in figure 1, except that $N = 3$; $k_x = 0$.

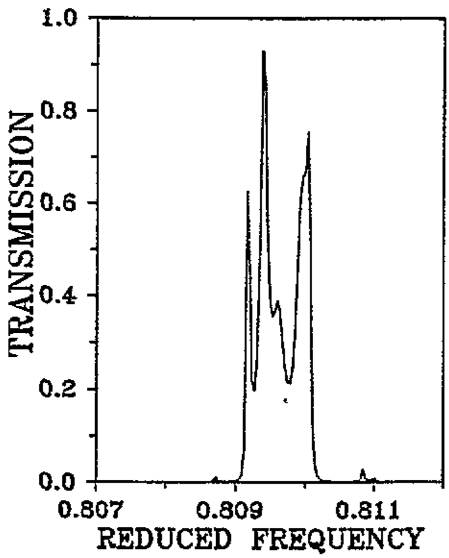

Figure 9. The transmission coefficient as a function of frequency in the absence of a magnetic field for the sample of parameters described in figure 1, except that $N = 10$; $k_x = 0$.

The calculated examples for the transmission coefficients of samples with the same degree of randomness but with different numbers of layers in the absence of magnetic field are plotted in figures 8 and 9. We only display the curves in a small region near a resonant frequency; the transmissions outside this region are vanishingly small, except near the other resonant frequencies. It can be seen that the resonant transmissions are certainly narrow with respect to the frequency even if the total number of layers in the superlattice is small. As a comparison, in figure 10 we plot the calculated result for a finite regular superlattice with a larger number of layers, where the transmission occurs over a much wider frequency region. The structure in the figures comes from the finiteness of the total number of layers of the samples, in which the band of an infinite superlattice reduces to discrete levels. The oscillation of the amplitudes of the peaks in figure 10 is due to the phase interference at the two ends of the superlattice, since we used different materials for A and C. The oscillation is not apparent for the random samples of figures 8 and 9 because the resonant region is much narrower in this case. The amplitude of the transmission, however, can be influenced by this phase interference.

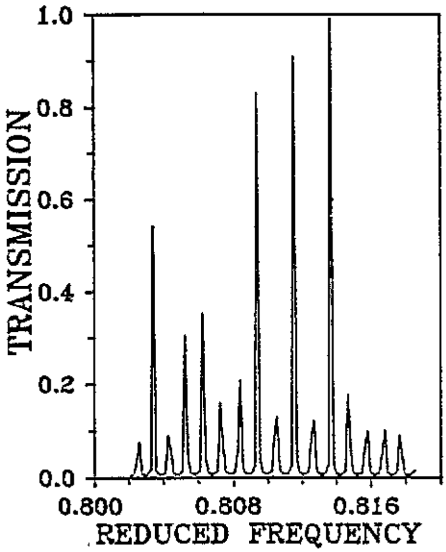

Figure 10. The transmission coefficient as a function of frequency in the absence of a magnetic field for a regular superlattice with $N = 20$ and $l_{ai} = L_a$ for $i = nm + 1$. The other parameters are the same as those in figure 7.

It is also interesting to investigate the dependence on the magnetic field of the transmission coefficients of the p-polarized waves at the resonant frequencies. Some examples are presented in figures 11 and 12. The transmission coefficients are very sensitive to the field strength. As the magnetic field increases, the transmissions are rapidly damped. This is because the cyclotrons change the dielectric functions of the conduction layers and the phases of the waves reflected at the interfaces, so condition (38) for the unscattered waves is no longer satisfied. The structures in the curves are also due to the finiteness of the total number of layers. By comparing the two figures, we can see that with increasing total number of layers, the damping becomes more rapid and the peaks become denser.

5. Summary

We have investigated the dispersion relations and the transmission coefficients of the magnetoplasmon polariton modes in a specially constructed random superlattice. Our

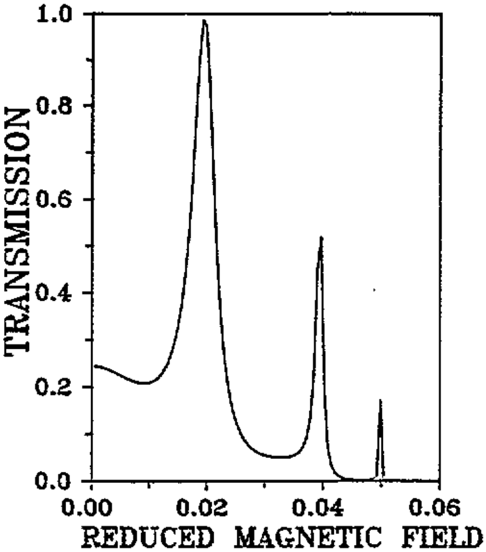

Figure 11. The transmission coefficient as a function of magnetic field for the sample of parameters described in figure 1, except that $N = 10$; $ck_x/\omega_p = 0.1667$ and $\omega/\omega_p = 0.81$.

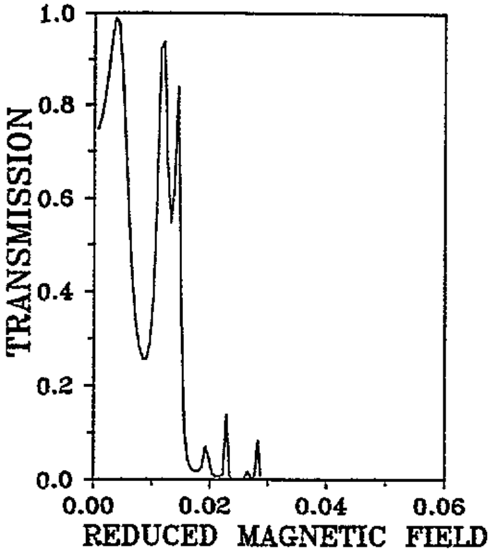

Figure 12. The transmission coefficient as a function of magnetic field. The parameters are the same as those in figure 10, except that $N = 50$.

purpose was to calculate the frequencies of the bulk modes, in particular to discover those modes that are completely unscattered by the randomness and that have finite transmissions. We took the magnetic field to be parallel to the interfaces and the incident plane of the EM waves to be perpendicular to the field. In such a highly symmetric geometry the formalism was simplified and the features of the system became easier to see.

We have shown that in a superlattice with partially random layer thicknesses of species A and regular layers of species B, a small portion of the bulk modes are unscattered in the random structure, although most of the modes are localized as expected from the scaling theory. This leads to an interesting feature of the system: high-quality resonant transmission. The resonance is certainly narrow in the frequency and is sensitive to the magnetic field. There seems to be the possibility of developing new devices, such as optical filters, magnetic-field sensors or electro-optical switches, by using this feature.

We have also found that there exists a mini-structure within the resonant region. It is caused by the finite number of layers of the superlattice. By increasing the number of layers, the peaks in the structure become denser. At the same time, the value of the transmission at the resonant frequency is influenced by the interference at the two ends of the finite superlattice. It may be interesting, in further investigations, to consider the effect of other physical factors, such as the damping of the carriers, on the detailed features of the resonant transmission.

Acknowledgment

This work was supported by the National Fund of Natural Sciences of China.

References

[1] Dow J, Ren S Y and Hess K 1982 *Phys. Rev.* B **25** 6218
[2] Kasu M, Yamamoto T, Noda S and Sasaki A 1990 *Japan. J. Appl. Phys.* **29** 828
[3] Yamamoto T, Kasu M, Noda S and Sasaki A 1990 *J. Appl. Phys.* **68** 5318
[4] Chen X S and Xiong S J 1993 *Phys. Rev.* B **47** 7146
[5] Abrahams E, Anderson P W, Liccirdello D C and Ramakrishnon T V 1979 *Phys. Rev. Lett.* **42** 673
[6] Dunlap D H, Wu H-L and Phillips P W 1990 *Phys. Rev. Lett.* **65** 88
[7] Xiong S J 1993 *Appl. Phys. Lett.* **63** 81
[8] Szenics R, Wallis R F, Giuliani G F and Quinn J J 1986 *Surf. Sci.* **166** 45
[9] Wallis R F, Szenics R, Quinn J J and Giuliani G F 1987 *Phys. Rev.* B **36** 1218
[10] Babiker M, Constantinou N C and Cottam M G 1987 *J. Phys. C: Solid State Phys.* **20** 4581
[11] Wallis R F and Quinn J J 1988 *Phys. Rev.* B **38** 4205
[12] Kushwaha M S 1989 *Phys. Rev.* B **40** 1692
[13] Kushwaha M S 1992 *Phys. Rev.* B **45** 6050
[14] Camley R E and Mills D L 1984 *Phys. Rev.* B **29** 1695
[15] Johnson B L, Weiler J T and Camley R E 1985 *Phys. Rev.* B **32** 6544
[16] Johnson B L and Camley R E 1986 *Solid State Commun.* **59** 595
[17] Wang P L and Xiong S J 1994 *Phys. Rev.* B **49** 10373
[18] Born M and Wolf E 1980 *Principles of Optics* 6th edn (Oxford: Pergamon) p 67
[19] Kohmoto M, Kadanoff L P and Tang C 1983 *Phys. Rev. Lett.* **50** 1870